Eur. Phys. J. D (2013) 67: 239
DOI: 10.1140/epjd/e2013-40319-7

THE EUROPEAN PHYSICAL JOURNAL D

Regular Article

Theoretical study of neutral bismuth-copper, bismuth-silver and bismuth-gold clusters

Eduardo Rangel and Luis Enrique Sansores[a]

Instituto en Investigaciones en Materiales, Universidad Nacional Autónoma de México, Apartado. Postal 70-360, C.P. 04510, México, D.F., Mexico

Received 24 May 2013 / Received in final form 6 September 2013
Published online 22 November 2013 –

Abstract. The study of alloy clusters is particularly interesting since the importance of the electronic and geometrical contributions to the stability can be investigated by examining the influences of substituting different atoms in a cluster. In this work we study the equilibrium geometries, relative stability, and electronic properties including the ionization energy (IE), electron affinity (EA), reactivity, aromaticity, and gap of small Bi_mCu_n(bismuth/copper) clusters and their cations with $m + n \leqslant 5$. The work is complemented with the study of small neutral bismuth/silver (Bi_mAg_n) and bismuth/gold (Bi_mAu_n) clusters. The study was done using density functional theory with the M06l functional. Comparison of neutral Bi_mCu_n clusters with the cationic $Bi_mCu_n^+$ and neutral Bi_mAg_n and Bi_mAu_n clusters show only small distortions of the geometries, except for $Bi_2Cu_2^+$, $Bi_1Cu_4^+$, $Bi_2Cu_3^+$, $Bi_3Cu_2^+$, $Bi_4Cu_1^+$, Bi_2Ag_2, Bi_3Ag, Bi_3Ag_2, Bi_2Ag_3, Bi_2Au_2, Bi_3Au and Bi_2Au_3. Our results on stability for cationic $Bi_mCu_n^+$ clusters are consistent with experimental report. The electronic affinity for odd number of total atoms of Bi_mCu_n, Bi_mAg_n and Bi_mAu_n increases with increasing number of copper, silver or gold atoms. Moreover, it is found that the Bi_mAu_n are more stable than Bi_mCu_n and Bi_mAg_n structures. Nuclear independent chemical shift analysis confirms the presence of *sigma* and *pi* aromatic/antiaromatic character.

1 Introduction

The study of alloy clusters is particularly interesting since the importance of the electronic and geometrical contributions to the stability can be investigated by examining the influences of substituting various atoms in a cluster [1–6]. If such exotic materials could be formed, they might well exhibit unique electronic, magnetic, optical, mechanical, and catalytic properties, and these could potentially lead to technological uses [7]. The interplay between isotropic (copper, silver or gold) interaction and directional bonds (bismuth) can be examined by studying bimetallic clusters. Previous papers, report theoretical and experimental studies of the stability of gold clusters doped with transition metal atoms (Sc, Ti, Cr, Fe) [8]. In other work, small SnBi clusters were investigated by employing the electric field deflection method [9]. Comparison of theoretical and experimental results enables identification of the growing patters of these small bimetallic clusters. It is well know that small gold, copper and silver cluster adopt planar structures for $n \leqslant 5$ atoms [10].

Yuan et al. [11] using DFT with Perdew and Wang correlation functional and Becke's exchange functional, studied neutral and cationic Bi_n clusters ($n = 2$–24). The structures found are similar to that of other group-V elemental cluster, extensive studies show that sizes with $n = 4$ and 8 have a tetrahedron and wedge like structures. They also found that larger Bi clusters have a tendency to be amorphous and are formed by combinations of Bi_4, Bi_6 and Bi_8 structures and for each cationic cluster the dissociation consist of Bi_4 and Bi_7^+ subclusters. This confirms that the subclusters are more stable than the larger Bi clusters. The HOMO-LUMO gap shows that Bi clusters would prefer a semiconductor character to metallicity. Kuznetsov et al. [12] studied bismuth polycationic clusters using Hartree Fock and DFT at B3LYP level with small and large ECP's. They found that there are some exceptions to Wade's rule and that several show a meta-stable behaviour.

There is only one experimental study of bismuth/copper clusters (Bi_mCu_n) produced by gas aggregation and investigated by time-of-flight mass spectrometry following ionization with a KrF excimer laser [13]. The measurements are done on cationic clusters. In their study most of their clusters have $m + n \leqslant 5$, only the $(m, n) = (2, 5)$ and (3,6) clusters outside this range have high intensities; signals for bigger clusters are small and in fact not identified. They show that in this system the magic numbers appear at $(m, n) = (1, 4)$, (2,5), (3,6) and (4,1). Two types of magic numbers are observed: those that reflect the stability of jellium shell closing by counting the total number of valence electrons from the component metals (where Cu atom donates one electron and Bi donates five electrons) and those where Wade's rule is predominant. However, up to now theoretical studies on Bi_mCu_n, Bi_mAg_n

[a] e-mail: sansores@unam.mx

Table 1. Calculated energy of formation (E_f) in eV and bond distances (d) in Å for binary alloys.

Alloy	E_f(ev)			d (Å)			
	CCSD	CCSDT	M06l	CCSD	CCSDT	M06l	Exp.
Cu_2	−1.70	−1.86	−2.02	2.284	2.268	2.230	2.19[21]
Ag_2	−1.37	−1.45	−1.90	2.627	2.621	2.570	2.53[22]
Au_2	−4.82	−4.91	−5.02	2.575	2.572	2.560	2.47[22]
Bi_2	−4.96	−5.38	−4.31	2.600	2.633	2.664	2.66[23]
BiCu	−1.82	−1.98	−1.75	2.489	2.473	2.460	
BiAg	−1.69	−1.81	−1.51	2.677	2.670	2.860	
BiAu	−3.82	−3.98	39.09	2.557	2.552	2.748	

and Bi_mAu_n clusters have not been realized to understand the geometric structures and electronic properties.

The aim of this work is to study the geometric structures, relative stability, and electronic structure including the ionization energy (IE), electron affinity (EA), reactivity and the HOMO-LUMO gap (highest occupied molecular orbital – lowest unoccupied molecular orbital) of small bismuth/cooper, bismuth/silver and bismuth/gold clusters and their cations with $m + n \leqslant 5$.

2 Computational procedures

Geometry optimizations were performed using density functional theory (DFT) method with meta-GGA M06l functional as implemented in Gaussian 09 code [14]. Effective pseudopotentials were included for the atom's core. The Stuttgart small core pseudopotential (PP) and basis were employed for Bi, which includes scalar relativistic and spin-orbit effects (SO) [15]. The basis set 6-31++G(d,p) was used for Cu and the SDD basis and pseudopotential were used for Ag and Au atom's [16]. The M06l functional is designed to capture the main dependence of the exchange-correlation energy on local spin density, spin density gradient and spin kinetic energy density; it is parameterized to satisfy the uniform electron gas limit and to have good performance for both main-group chemistry and transition metal chemistry [17].

To scan the conformational space we evaluated the quantum energy of 32 randomly generated candidate structures for each type of alloy. The random search was carried out using ASCEC program [18], which contains an adapted version of the simulated annealing optimization algorithm. No symmetry restrictions were imposed in the process of geometry optimization. Frequency analyses were performed to check that the optimized structures are true local minima on the potential energy surface.

For the formation energy of neutral Bi_mCu_n,Bi_mAg_n and Bi_mAu_n we used $E_f = E(Bi_mM_n) - [mE(Bi) + nE(M)]$ and for cationic $Bi_mCu_n^+$, $Bi_mAg_n^+$ and $Bi_mAu_n^+$ clusters, $E_f = E(Bi_mM_n^+) - [(n-1)E(M) + E(M^+) + mE(Bi)]$, where $E(Bi_mM_n)$, $E(Bi_mM_n^+)$ are the energies of the final optimized structures; $mE(Bi) + nE(M)$ is the sum of the energy of Bi atoms and the metal atoms with no interaction between them; M is Cu, Ag or Au. $E(M^+)$ is the energy of M cation since we considered that the positive charge is on the dopant atom (Cu, Ag or Au) since this atom has the lowest electronegativity.

We also calculated the condensed Fukui function to study the reactivity of different sites in the clusters. Fukui functions are defined as: $f_k^- = q_k(N) - q_k(N-1)$ and $f_k^+ = q_k(N+1) - q_k(N)$, where $q_k(N)$, $q_k(N-1)$ and $q_k(N+1)$ are the NBO charge on atom k for N total electrons, $N+1$ with an electron added and $N-1$ with an electron removed to the neutral cluster.

To test our results with M06l functional we have also optimized the structure of the binary and ternary alloys with CCSD [19–22] and CCSDT [23]. Since CCSDT is computationally very expensive only the minimum energy structures were calculated. In Table 1 the energy of formation and structure parameters are given, available experimental values are included. For the binary alloys the M06l calculated bond length is in better with the experimental values agreement than CCSD or CCSDT; the standard deviation of the bond length for M06l is 0.031 Å while that for CCSDT is 0.052 Å. The standard deviation between M06l and CCSDT for all binary alloys 0.098 Å and the bigger difference of 0.2 Å is for BiAu and BiAg. The Bi_2, Cu_2, Ag_2 and Au_2 experimental vibrational frequencies 173.1 cm^{-1} [24], 264.5 cm^{-1} [25], 192 cm^{-1} [25] and 190.9 cm^{-1} [26], respectively, are in good agreement with our calculated values with M06l 177 cm^{-1}, 268.1 cm^{-1}, 195 cm^{-1} and 213.5 cm^{-1}, respectively. In general the formation energy is in good agreement for all calculations except for Au_2. For Au_2 the energy of formation calculated with M06l is positive and very large, while for both CCSD and CCSDT is negative with a reasonable value; it should be notice that for M06l in order to get convergence we had to use the quadratic convergence procedure of g09. Nevertheless, the bond lengths and vibrational frequencies are in good agreement with the experiment and with CCSDT calculations.

In Table 2 the same data is shown, with the addition of one angle. Since all structures are isosceles triangles the angle included is that between the equal sides. It should be notice that the energy of formation follows the same trend for both CCSD and M06l and that always the triangular structure is more stable than the best linear structure. CCSDT and M06l also follow the same trend; in fact, the standard deviation in the energy of formation difference is only 0.1 eV. In terms of structure the bond lengths are very similar, the standard deviation is only 0.046 Å and

Table 2. Calculated energy of formation (E_f) in eV and bond distances (d) in Å and angles (°) for ternary alloys. Tr denotes the triangular structure and L the linear one. Linear alloys Bi_2Cu and Bi_2Au were not a minimum.

Alloy	E_f(ev)			d(Å)			Angle (°)		
	CCSD	CCSDT	M06l	CCSD	CCSDT	M06l	CCSD	CCSDT	M06l
Bi_3	−8.23	−8.63	−7.2	2.826	2.825	2.890	63.58	64.00	63.96
Cu_3	−2.59	−2.92	−2.52	2.344	2.326	2.230	68.81	67.40	60.04
$BiCu_2$-Tr	−4.63	−4.97	−4.17	2.513	2.506	2.503	64.26	62.10	59.06
$BiCu_2$-L	−2.39		−3.18	2.547		2.520	180.0		180.0
Bi_2Cu-Tr	−6.24	−6.72	−5.93	2.599	2.579	2.562	64.16	65.72	68.27
Bi_2Cu-L									
Ag_3	−2.08	−2.26	−1.80	2.856	2.691	2.680	55.22	67.61	60.00
$BiAg_2$-Tr	−4.35	−4.57	−3.65	2.700	2.696	2.717	69.10	67.97	64.20
$BiAg_2$-L	−2.14		−2.24	2.759		2.780	180.0		180.0
Bi_2Ag-Tr	−5.99	−6.41	−5.57	2.816	2.810	2.807	58.65	59.67	61.29
Bi_2Ag-L	−5.04		−4.62	3.321		3.020	180.0		180.0
Au_3	−7.37	−7.55	−7.20	2.620	2.614	2.660	122.8	122.69	121.4
$BiAu_2$-Tr	−8.46	−8.73	−7.48	2.590	2.588	2.651	77.72	74.62	73.26
$BiAu_2$-L	−5.95		−3.40	2.651		2.720	180.0		180.0
Bi_2Au-Tr	−7.53	−7.92	−6.21	2.730	2.719	2.761	62.09	63.04	63.42
Bi_2Au-L									

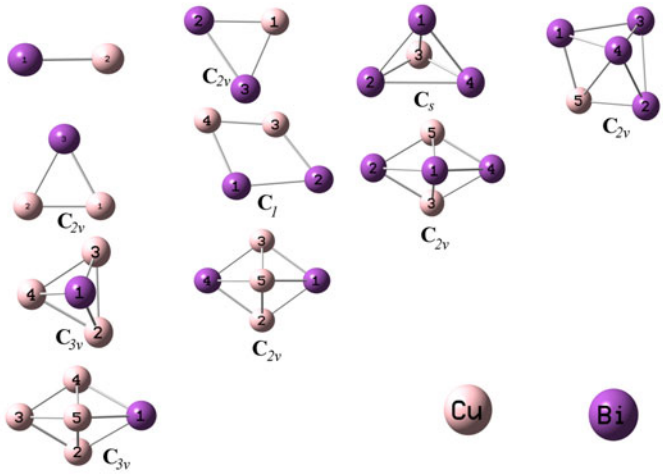

Fig. 1. Lowest-energy structures for neutral Bi_mCu_n, with $m + n \leqslant 5$.

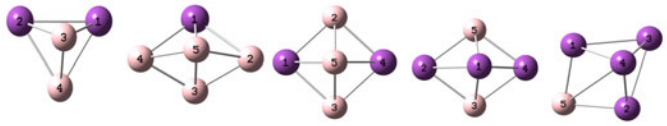

Fig. 2. Lowest-energy structures of $Bi_2Cu_2^+$, $BiCu_4^+$, $Bi_2Cu_3^+$, $Bi_3Cu_2^+$ and $Bi_4Cu_1^+$. All structures have C_{2v} symmetry.

the same for angles is 3.29°, which is smaller than that for CCSD-CCSDT (4.11°).

The previous analysis shows that M06l is a reliable functional for this clusters and that results can be used with confidence.

3 Results and discussion

3.1 Geometries of neutral and cationic Bi_mCu_n clusters

The lowest-energy structures for neutral Bi_mCu_n and $Bi_mCu_n^+$, for $m + n \leqslant 5$, optimized with M06l functional are shown in Figures 1 and 2, respectively. Pure Bi clusters have 3D structures while Cu clusters have planar structures in agreement with previous DFT calculations [11,27,28]. In general, the Bi_mCu_n clusters have 3D structures only the Bi_2Cu_2 is planar. From Figure 1 we can also see that there is some kind of symmetry when interchanging Bi by Cu; in other words, the structure of Bi_mCu_n is similar to that of Bi_nCu_m. Most structures have C_{2v} symmetry, only two of them $BiCu_3$ and $BiCu_4$ have C_{3v} symmetry and Bi_2Cu_2 has no symmetry. It would be expected that Bi_3Cu and Bi_4Cu would also have a three-folded symmetry but in both cases the copper ion does not like to be bonded to 3 bismuth atoms, it is only bonded to 2 (for data associated with bond lengths (Å) and angles (°), see the Appendix).

The lowest energy structure corresponds to their lowest spin states; in some cases the energy difference with the triplet state is very small. When we compared our results for neutral clusters with the cationic clusters, we find small changes, with slight distortions in the structures, except for $Bi_2Cu_2^+$, $Bi_1Cu_4^+$, $Bi_2Cu_3^+$, $Bi_3Cu_2^+$ and $Bi_4Cu_1^+$ where the structure is different as shown in Figure 2. The big change is in the Bi_2Cu_2 where the neutral is planar but the cation is 3D. Cluster $Bi_1Cu_4^+$ changes symmetry group from C_{3v} to C_{2v}. The same behaviour mention above with respect to the interchange of Bi by Cu is seen.

Yamada et al. [13] found the magic numbers for the metal alloy clusters $Bi_mCu_n^+$: (1,4), (4,1), (5,2), and (6,3). The first 2 are explained in terms of the jellium model and the last 2 by Wade's rules. The magic numbers refer to those clusters that are more abundant which should imply that they are more stable. This means that there

Table 3. Electronic properties of neutral Bi_mCu_n, with $n = 1-5$, $m = 1-5$ and $m + n \leqslant 5$: formation energy (eV), HOMO-LUMO gap (eV), ionization energy (eV), electron affinity (eV) and electrical dipole (Debye).

System	Formation energy	Formation energy per atom	Energy gap	Ionization energy	Electron affinity	Dipole
BiCu	−1.75	−0.88	0.41	−6.65	2.10	0.84
Bi_2Cu	−5.93	−1.98	0.57	−6.31	1.20	0.57
$BiCu_2$	−4.17	−1.39	0.84	−6.40	2.24	1.84
Bi_3Cu	−9.18	−2.30	0.60	−6.35	1.52	0.95
Bi_2Cu_2	−8.16	−2.04	1.08	−6.62	1.25	0.62
$BiCu_3$	−7.80	−1.95	1.70	−7.03	1.00	1.26
Bi_4Cu	−13.2	−2.64	1.83	−6.15	1.56	0.52
Bi_3Cu_2	−11.8	−2.36	0.71	−6.48	1.86	1.03
Bi_2Cu_3	−10.7	−2.14	0.85	−6.64	1.84	0.21
$BiCu_4$	−9.73	−1.95	1.66	−6.76	2.00	1.39

Table 4. Properties cationic clusters $Bi_mCu_n^+$. The formation energy (eV), HOMO-LUMO gap (eV) and electrical dipole (Debye).

System	Formation energy (Cu cation)	Formation energy per atom	Energy gap	Dipole
$BiCu^+$	−2.70	−1.35	0.14	2.26
Bi_2Cu^+	−7.32	−2.44	1.88	2.41
$BiCu_2^+$	−5.57	−1.86	0.45	2.62
Bi_3Cu^+	−10.67	−2.67	0.44	1.54
$Bi_2Cu_2^+$	−9.58	−2.40	0.39	2.15
$BiCu_3^+$	−8.43	−2.10	2.25	3.12
Bi_4Cu^+	−15.32	−3.06	2.35	2.26
$Bi_3Cu_2^+$	−13.20	−2.64	1.00	0.31
$Bi_2Cu_3^+$	−11.82	−2.36	0.17	1.03
$BiCu_4^+$	−11.67	−2.33	2.10	2.61

should be some correlation with the formation energy. In fact there should be some correlation between the intensities measured by Yamada et al. and the calculated formation energy. In Tables 3 and 4 the formation energies of the neutral and cation clusters are given. For the charged clusters we have computed the formation energy assuming that the charged ion could either be a Cu or a Bi. Both show the same behaviour so we will only refer to the first one. To begin, the intensity for Bi_2Cu^+ is greater than that of $BiCu_2^+$, the formation energies follows the same behaviour 7.32 eV and 5.57 eV.

Similarly, in the series of 4 atoms, $Bi_2Cu_2^+$ has approximately the same intensity than $Bi_3Cu_1^+$ and $BiCu_3^+$, the corresponding formation energies are 9.58, 10.67 and 8.43 eV, respectively. Finally, for the series of 5 atoms, $Bi_4Cu_1^+$ has higher intensity (15.32 eV) than $Bi_1Cu_4^+$ (11.67 eV) and $Bi_3Cu_2^+$ (13.20 eV), the formation energies follow the same trend.

On the other hand, we find that the neutral structures are less stable than the cationic structures (cations have a higher formation energy than neutral clusters), as shown in Tables 3 and 4. Assuming that the Cu atom donates one electron and Bi donates five electrons to the cluster, the total number of valence electrons in Bi_mCu_n is given by $5m+n$. The clusters with even number of atoms $m+n$ have even numbers of electrons. If we divide the formation energy by the number of atoms corresponding to its stoichiometry and compare the results, we find that the clusters with even number of atoms are as stable as the neighbouring clusters having odd number of atoms.

3.2 Orbitals

Tables 3 and 4 show that the electric dipole and the HOMO-LUMO gap oscillate as the cluster size increases. The vertical IE is calculated as $IE = E_n^+ - E_n$, where E_n^+ is the total energy of the cationic cluster with the neutral geometry and the vertical EA is calculated from $EA = E_n - E_n^-$, where E_n^- is the total energy of the anion with the neutral geometry. Table 3 shows the calculated IEs and EAs. The IEs of Bi_mCu_n clusters are approximately independent of size or number of atoms. However, the EA of the neutral clusters increases with increasing number of copper atoms; we find the following behaviour:

$$\begin{aligned} &EA(Bi_2) < EA(BiCu) < EA(Cu_2),\\ &EA(Bi_3) < EA(Bi_2Cu) < EA(BiCu_2) < EA(Cu_3),\\ &EA(Bi_4) < EA(BiCu_3) < EA(Bi_2Cu_2)\\ &\qquad < EA(Bi_3Cu) < EA(Cu_4) \end{aligned}$$

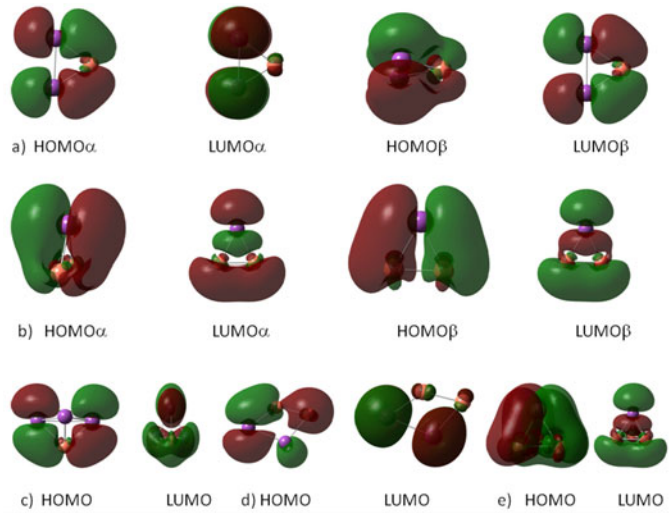

Fig. 3. Spatial representation of the HOMO and LUMO of compounds: (a) Bi_2Cu, (b) $BiCu_2$, (c) Bi_3Cu, (d) Bi_2Cu_2 and (e) $BiCu_3$.

and

$$EA(\mathrm{Bi_5}) < EA(\mathrm{Cu_5}) \sim EA(\mathrm{Bi_4Cu}) < EA(\mathrm{Bi_2Cu_3}) \sim EA(\mathrm{Bi_3Cu_2}) < EA(\mathrm{BiCu_4}).$$

This is expected since Cu is less electronegative than Bi and indicates that metallicity is lost as the number of Bi increases.

The HOMO and LUMO orbitals of Bi_2Cu, $BiCu_2$, Bi_3Cu, Bi_2Cu_2 and $BiCu_3$ are shown in Figure 3. All these orbitals are formed with main contributions from the $6p$ orbitals of the bismuth and the $3d$ of the Cu. For compound Bi_2Cu the HOMO alpha is antibonding with b_2 symmetry and the LUMO alpha also antibonding has a_2 symmetry. The HOMO beta has b_1 symmetry, it is a bonding orbital between al three atoms. The LUMO beta is b_2 and is antibonding between the bismuth atoms and bonding for the Cu atoms with both Bi atoms. For compound $BiCu_2$ the situation is completely different, both HOMOs are bonding, HOMO alpha with b_1 symmetry bonds all three ions, while HOMO beta with b_2 symmetry bonds the Cu ions with the bismuth but is antibonding between coppers; both LUMOs are very similar the alpha with a_1 symmetry and the beta with b_1.

The set of compounds with 4 ions is closed shell so we only have one HOMO and one LUMO. Compound Bi_3Cu has a HOMO with a'' symmetry and LUMO with a' symmetry. The HOMO is bonding between the Cu and 2 bismuths and antibonding between bismuths, in fact there is one bismuth ion that does not participate; even more, in the LUMO this ion shows a dangling bond. Compound Bi_2Cu_2 should be a fairly unstable compound the HOMO shows very poor bonding character and the LUMO is antibonding. Finally compound $BiCu_3$ that has C_{3v} symmetry, with a HOMO that bonds every thing together, is doubly degenerated with symmetry e and the LUMO with a_1 symmetry has contributions from all four ions. This should be a fairly stable compound with an aromatic character.

To determine the nature of bonding in Bismuth/copper clusters, NBO population analyses calculations and molecular orbital analyses were performed. The delocalized molecular orbitals of all studied systems are alike. These facts indicate that the Bi-Bi and Bi-Cu bonding in Bi_mCu_n clusters has a covalence character, while the Cu-Cu has a metallic character.

Table 5. Fukui functions for neutral Bi_mCu_m clusters. Symmetric atoms are not included.

Cluster	Atom	f^+	f^-
BiCu	Cu	0.61	0.52
	Bi	0.39	0.48
Bi_2Cu	Cu1	0.23	0.23
	Bi2	0.38	0.38
$BiCu_2$	Cu1	0.18	0.21
	Bi3	0.65	0.58
Bi_3Cu	Cu3	0.16	0.16
	Bi1	0.33	0.14
	Bi3	0.25	0.35
Bi_2Cu_2	Cu3	0.11	0.14
	Cu4	0.19	0.34
	Bi1	0.31	0.10
	Bi2	0.39	0.42
$BiCu_3$	Cu2	0.21	0.07
	Bi1	0.37	0.46
Bi_4Cu	Cu5	0.15	0.09
	Bi1	0.30	0.32
	Bi3	0.13	0.13
Bi_3Cu_2	Cu3	0.07	0.07
	Bi1	0.12	0.12
	Bi2	0.10	0.64
Bi_2Cu_3	Cu2	0.02	0.03
	Cu5	0.13	0.14
	Bi1	0.41	0.40
$BiCu_4$	Cu3	0.40	0.44
	Cu2	0.08	0.07
	Bi1	0.38	0.36

3.3 Reactivity of neutral Bi_mCu_n clusters and electronic properties

The condensed Fukui function can give, in general, valuable information about the site selectivity in chemical reactions and systematization in a family of clusters [29]. Table 5 shows the Fukui coefficients for lowest-energy structures of neutral Bi_mCu_n, with $m + n \leqslant 5$.

The function f^+ is associated with LUMO and measures reactivity toward a donor reagent and f^- is associated with HOMO and measures reactivity toward an acceptor reagent. An analysis of the most reactive clusters shows that Bi_3 cluster presents three active sites, two nucleophilic centres and the other Bi is an electrophilic centre, while Cu_3 presents two electrophilic centres. In BiCu, Bi is the most active centre and Cu is less active for both nucleophilic and electrophilic attacks. In $BiCu_2$ the most

Table 6. Calculated NICS at the centre of the cluster.

Cluster (m,n)	$Bi_mCu_n^+$	Bi_mCu_n	Bi_mAg_n	Bi_mAu_n
(1,2)	55.92	23.95	14.89	−52.24
(2,1)	28.40	7.89	32.23	−132.39
(1,3)	273.16	52.17	42.47	34.95
(2,2)	51.01	−98.84	296.91	−776.02
(3,1)	2.08	12.09	18.35	11.41
(1,4)	49.95	41.45	24.82	21.22
(2,3)	−38.78	22.73	11.11	24.68
(3,2)	21.45	5.84	16.24	34.15
(4,1)	48.37	27.81	38.19	−0.65

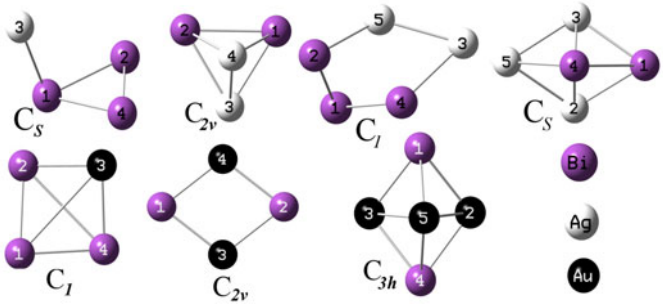

Fig. 4. Lowest-energy structures for neutral for Bi_3Ag, Bi_2Ag_2, Bi_3Ag_2, Bi_2Ag_3, Bi_3Au, Bi_2Au_2 and Bi_2Au_3.

active centre would be Bi for both electrophilic and nucleophilic attack (see Tab. 5 and Fig. 3). Bi_2Cu shows less activity. For the cluster series with $m+n=4$, Bi sites are more reactive, while Cu sites are almost non reactive. In Bi_3Cu two Bi sites are nucleophilic and one electrophilic; in Bi_2Cu_2 there is some electrophilic reactivity at the Cu site; and in $BiCu_3$ (see Tab. 5 and Fig. 3), Bi shows nucleophilic and electrophilic reactivity. Finally for the series $m+n=5$, Bi_3Cu_2 shows very high electrophilic reactive sites at the Bi atoms, while Cu sites are reactive only in the $BiCu_4$.

In general we can conclude that in these clusters the Cu sites have very low reactivity, while Bi sites are more reactive to nucleophilic and electrophilic attack. Increasing the number of Bi reduces the activity those sites.

In the following section we will discuss the properties of neutral bismuth/silver and bismuth/gold clusters.

3.4 Neutral bismuth/silver and bismuth/gold clusters

We have also studied neutral Bi_mAg_n and Bi_mAu_n. In all cases the lowest energy structure corresponds to their lowest spin state. From a structural point of view the structures of these clusters are almost the same than those of Bi_mCu_n discussed above, including the symmetry, except for: Bi_3Ag, Bi_2Ag_2, Bi_3Ag_2, Bi_2Ag_3, Bi_2Au_2, Bi_3Au and Bi_2Au_3 whose structures are shown in Figure 4 (for data associated with bond lengths (Å) and angles (°), see the Appendix).

In the case of Bi_3Ag, silver is only bonded to one Bi, while in Bi_3Cu, the copper bonds to the three Bi atoms. For Bi_3Cu_2 and Bi_3Cu we have a 3D structure while Bi_3Ag_2 and Bi_3Au are planar; on the other hand Bi_2Cu_2 cluster is planar while Bi_2Ag_2 has a pyramidal structure and Bi_2Au_2 is planar but has a symmetrical structure. This behaviour is probably a steric effect since Cu and Au are smaller than silver.

In Figure 5 we compare Bi_mCu_n, Bi_mAg_n and Bi_mAu_n energy of formation, HOMO-LUMO gap, IE (ionization energy) and EA (electronic affinity). The behaviour of the IE is similar for all three transition metals clusters. The extremely high IE (see Fig. 5c) and low EA in compound (1,3) confirm the stability of Bi_1Cu_3, Bi_1Ag_3 and Bi_1Au_3, all with pyramidal structures. The EA for all three alloys increases with increasing number of transition metal atoms, only for odd number of total atoms. Finally compound (1,2) has the highest EA and (1,3) the lowest.

From the formation energy, we find that the Bi_mAu_n structures are more stable than Bi_mCu_n and Bi_mAg_n structures in all series, as is shown in Figure 5a. The expansion of the $5d$ orbitals probably contributes substantially to increase the binding energy of the open $5d$-shell transition metal clusters by making these orbitals more accessible. In general we can see that the formation energy for Bi_mCu_n and Bi_mAg_n clusters decreases with number of copper or silver atoms, respectively, while in the case of Bi_mAu_n cluster the general trend is to increase with the number of gold atoms.

Figure 5b shows that the HOMO-LUMO gap oscillates with the number of copper, silver and gold atoms. In the case of Bi_mCu_n and Bi_mAu_n, the results suggest that the clusters would like to be semiconductor rather than metallic. In contrast, for Bi_2Ag_2 cluster has a small HOMO-LUMO gap of 0.05 eV. The Bi_2Ag_2 cluster has a pyramidal structure, its electronic orbitals are delocalized and it is an antiaromatic compound. In the case of Bi_mAg_n clusters, we find that BiAg presents one nucleophilic centre (Bi atom) and Bi_3Ag cluster has one nucleophilic centre (Ag atom). The other clusters have very low reactivity centers. For Bi_mAu_n, the cluster with the more reactive site is BiAu that has one electrophilic centre (Bi atom). The Bi_3Au cluster has one nucleophilic centre (Bi_3 atom) and $BiAu_4$ has one electrophilic centre (Au_3 atom). The other clusters have less reactive sites.

From NBO population analysis, we find that in the Bi_mAg_n clusters there is an electronic charge transfer from the Ag atom to the Bi atoms. In contrast, Bi_mCu_n and Bi_mAu_n there is electronic charge transfer from the Bi atoms to the Au or Cu atoms. For example for Bi_4Ag, we found that the Ag atoms have a net positive charge +0.154. For Bi_4Cu and Bi_4Au clusters case, Cu and Au atoms have a net negative charge −0.025 and −0.117, respectively. The results for the reactivity in the clusters are a consequence of the charge transfer from the alpha and beta virtual and occupied orbitals available (LUMO and HOMO). An analysis of the reactivity shows that Bi_4Ag and Bi_4Cu clusters have less reactive sites. In contrast,

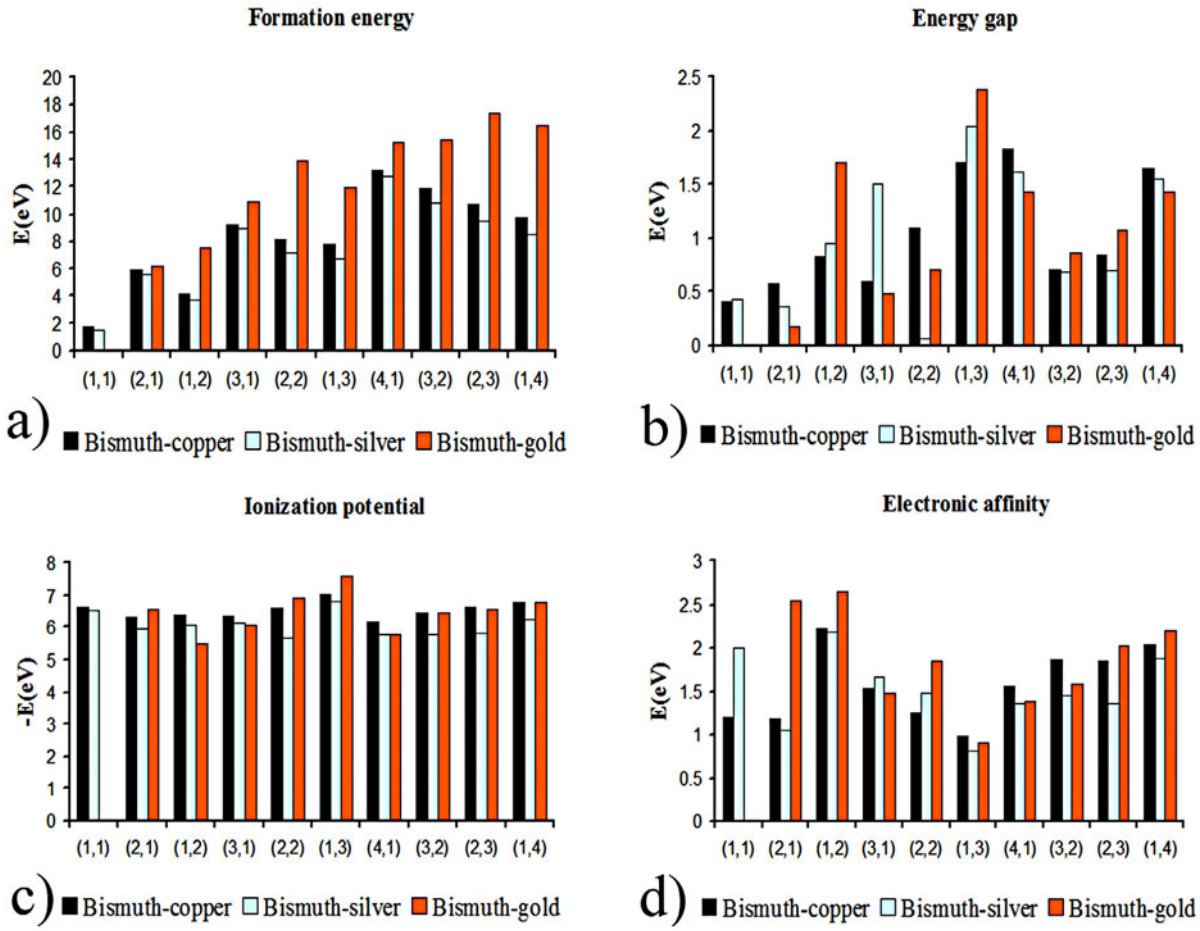

Fig. 5. Comparison between neutral bismuth/copper, bismuth/silver and bismuth/gold clusters. (a) Formation energy, (b) energy gap, (c) ionization energy, (d) electronic affinity.

Bi_4Au cluster presents one active site at the Au atom (nucleophilic centre).

The density of states (DOS) can help understand the above-mentioned behaviour (Fig. 6). The value of the total DOS for lowest alpha and beta virtual orbitals available is 2, 8 and 4 states/eV for Bi_4Cu, Bi_4Ag and Bi_4Au, respectively (see Fig. 6). However, for Bi_4Au there are two consecutive alpha virtual orbital available next to two consecutive beta virtual orbitals available. The LUMO alpha is an anti-bonding orbital between unoccupied gold s orbital and neighboring Bi p orbitals; the LUMO beta is a bonding orbital between unoccupied gold d orbital and neighboring Bi p orbitals. For Bi_4Cu, the energy gap between HOMO alpha and HOMO beta is 0.5 eV and 0 between LUMO alpha and LUMO beta (see Fig. 6). For Bi_4Ag, the energy gap between HOMO alpha and HOMO beta is 0.4 eV and 0.2 between LUMO alpha and LUMO beta. For Bi_4Cu and Bi_4Ag, both LUMO alpha and beta are anti-bonding between unoccupied Bi p orbitals. This indicates that Bi_4Ag has the biggest HOMO-LUMO gap so it should be the less reactive. Bi_4Au is more reactive than Bi_4Cu due to the contributions of s and d gold orbitals.

An analysis of the reactivity shows that $BiAu_4$ and $BiCu_4$ have more reactivity sites than $BiAg_4$ being the Au_3 and Cu_3 the most reactive sites. Figures 6b, 6d and 6f show the DOS for these compounds. For $BiCu_4$, $BiAu_4$ and $BiAg_4$ clusters, the value of the total DOS for alpha and beta virtual orbitals available is 4, 4 and 4 states/eV, respectively (see Fig. 6). Again $BiAg_4$ has the biggest HOMO-LUMO gap and is less reactive. On the other hand the available states for the Cu and Au are analogous and their reactivity is similar. In this case the frontier orbitals of all three compounds are comparable and thus their behaviour is alike.

3.5 Aromatic/antiaromatic metal clusters

It is always interesting to analyse the aromatic character of close ring clusters; it gives information about delocalized electrons and stability of the cluster. To calculate the aromatic character we used the nuclear independent chemical shift (NICS) procedure [30], and the GIAO method (Gauge Independent Atomic Orbital) to calculate the magnetic susceptibility [31] at the centre of the ring (see Tab. 4). Negative NICS denote an aromatic

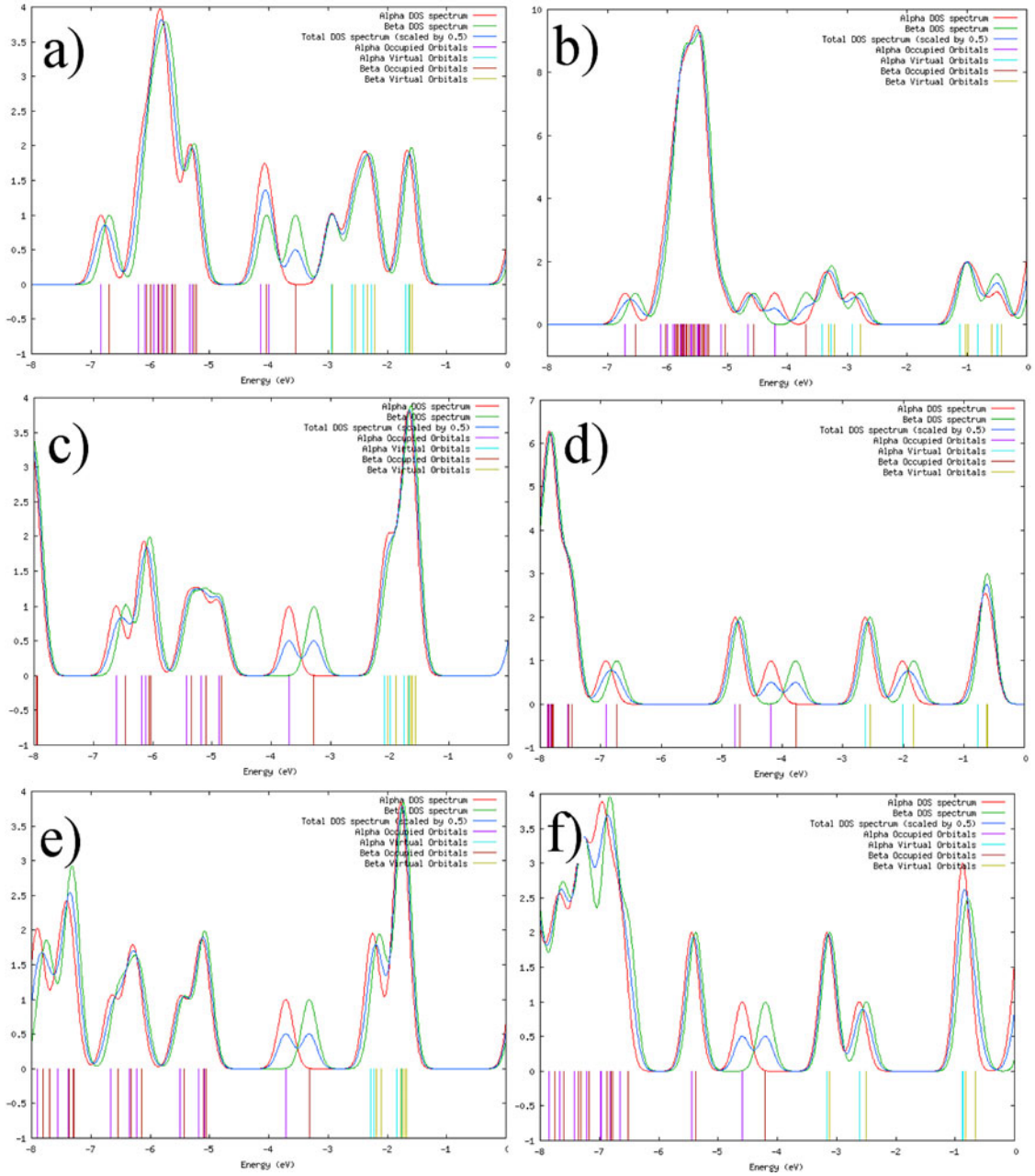

Fig. 6. Density states (DOS). (a) Bi_4Cu, (b) $BiCu_4$, (c) Bi_4Ag, (d) $BiAg_4$, (e) Bi_4Au and (f) $BiAu_4$.

character, whereas positive NICS denote antiaromatic behaviour [32]. Li et al. [33] using DFT have shown that only Bi_5^- cluster is aromatic, forms a planar ring and satisfies the Hükcel rule of $4n + 2\,\pi$ electrons. The NICS analysis suggests that the aromaticity for Bi_5^- arises primarily from the contributions of Bi-Bi σ bonds and Bi-Bi π bonds, while the aromaticity of Bi_5M (M = Li, Na, K) and Bi_5M^+ (M = Be, Mg, Ca) mainly owe to the Bi-Bi σ bonds [33]. In other work on bismuth polycation species, calculations were performed at the Hartree-Fock and density functional theory [12]. The bonding in bismuth polycations is characterized by a high degree of electron delocalization and three-dimensional aromaticity. In our systems, most of the compounds have an antiaromatic character, except for Bi_2Cu_2, Bi_2Au, $BiAu_2$ and Bi_2Au_2 with NICS value of -98.8, -132.4, -52.2 and -776.0, respectively. It is to be notice that most Cu and all Ag clusters have an antiaromatic character, which normally is an indication of instability, while some Au clusters have an aromatic character. We only find an aromatic character in those clusters that are flat and based on gold. In fact this is clear in the case of clusters with $(m, n) = (2, 2)$ where the regular shape gold based has the higher aromaticity and the 3D silver based cluster is anti aromatic. For Bi_2Au, $BiAu_2$ and Bi_2Au_2 we find two contributions to the current, one due to *pi* electrons and another to *sigma* electrons. The combination of

sigma and *pi* ring current confirms the multiple aromatic characters of these compounds.

4 Conclusions

In summary, the equilibrium geometries, relative stability, and electronic properties including the ionization energy (IE), electron affinity (EA), reactivity, aromaticity/antiaromaticity and HOMO-LUMO gaps of small bismuth/cooper (Bi_mCu_n) clusters and their cations with $m+n \leqslant 5$, were investigated using DFT method under the framework of the M06l functional. The work is complemented with the study of small neutral bismuth/silver and bismuth/gold clusters. When we compared our results for neutral clusters with the cationic $Bi_mCu_n^+$ clusters, we find only slight distortion of the structures, except for $Bi_2Cu_2^+$, $Bi_1Cu_4^+$, $Bi_2Cu_3^+$, $Bi_3Cu_2^+$ and $Bi_4Cu_1^+$. Our results on stability for cationic $Bi_mCu_n^+$ clusters are consistent with experimental report. It is found that the neutral structures are less stable than the cationic structures in the case of bismuth/cooper clusters.

On the other hand, results for neutral Bi_mCu_n clusters were compared with those for Bi_mAg_n and Bi_mAu_n clusters. For most clusters only slight distortions in the structures were found except for Bi_3Ag, Bi_2Ag_2, Bi_3Ag_2, Bi_2Ag_3, Bi_2Au_2, Bi_3Au and Bi_2Au_3. The IE behaviour of Bi_mAg_n and Bi_mAu_n is similar to that of Bi_mCu_n clusters. For odd total number of atoms, the EA increases with increasing number of copper, silver or gold atoms. Moreover, we find that the Bi_mAu_n structures are more stable than those of Bi_mCu_n and Bi_mAg_n. In the case of Bi_mCu_n and Bi_mAu_n, the results suggest that the clusters would like to be semiconductor rather than metal. Molecular orbital analysis and the application of the NICS index confirm the presence of *sigma* and *pi* aromatic/antiaromatic character. Most of the compounds have an antiaromatic character, except for Bi_2Cu_2, Bi_2Au, $BiAu_2$ and Bi_2Au_2. For Bi_2Au, $BiAu_2$ and Bi_2Au_2 which have an aromatic character. We find two contributions to the current, one due to *pi* electrons and another to *sigma* electrons. The combination of *sigma* and *pi* ring current confirms the multiple aromatic characters of these compounds. Finally, the bismuth/cooper clusters have more reactive sites than clusters of bismuth/silver and bismuth/gold.

Although the general behaviour for the three systems is similar there are some important differences: Bi_mAu_n clusters are more stable and aromaticity is more important, Bi_mAg_n shows are less reactive and Bi_mCu_n has more reactive sites. Our results also indicate that Bi bonds better with Au.

This research has received funding from the European Community Seven Framework Programme (FP7-NMP-2010-EU-MEXICO) and CONACYT under grant agreements 263878 and 125141, respectively. We thank the Computing and Information Technology Division of the UNAM for the computer resources and the Dirección General de Asuntos del Personal Académico for financial support (E. Rangel's scholarship).

Appendix: Data associated with bond lengths (Å) and angles (°) of the bismuth/cooper, bismuth/silver and bismuth/gold clusters

Table A.1. Bond lengths (Å) and angles (°) of the neutral clusters under study after optimization.

Cluster (Sim)	Bond	Length	Angle	
$Bi_2Cu(C_{2v})$	Bi2-Cu1	2.562	Bi2-Cu1-Bi3	68.3
$BiCu_2(C_{2v})$	Bi3-Cu1	2.503	Cu1-Bi3-Cu2	59.1
$Bi_3Cu(C_s)$	Bi1-Bi2	2.946	Cu3-Bi1-Bi2	52.0
	Bi1-Cu3	2.812	Bi4-Bi1-Bi2	76.4
			Bi4-Bi1-Bi2-Cu3	−52.1
$Bi_2Cu_2(C_1)$	Bi1-Bi2	2.897	Cu3-Bi1-Bi2	54.1
	Bi1-Cu3	2.652	Cu4-Bi1-Bi2	108.0
	Bi1-Cu4	2.627	Cu4-Bi1-Bi2-Cu3	0.0
$BiCu_3(C_{3v})$	Bi1-Cu2	2.531	Cu3-Bi1-Bi2	58.3
			Cu4-Bi1-Bi2-Bi3	69.9
$Bi_4Cu(C_{2v})$	Bi1-Bi2	4.065	Bi3-Bi1-Bi2	48.1
	Bi1-Bi3	3.044	Cu5-Bi1-Bi4	78.9
	Bi1-Cu5	2.568	Cu5-Bi1-Bi4-Bi2	−24.8
			Bi4-Bi1-Bi2-Bi3	84.8
$Bi_3Cu_2(C_{2v})$	Bi1-Bi2	3.044	Cu3-Bi1-Bi2	53.5
	Bi1-Cu3	2.768	Bi4-Bi1-Bi2	96.5
			Bi4-Bi1-Bi2-Cu3	33.9
			Cu5-Bi1-Bi2-Cu3	67.9
$Bi_2Cu_3(C_{2v})$	Bi1-Cu2	2.567	Cu3-Bi1-Cu2	75.5
	Bi1-Bi4	4.042	Bi4-Bi1-Cu2	38.1
	Bi1-Cu5	2.670	Cu5-Bi1-Cu2	56.7
			Bi4-Bi1-Cu2-Cu3	8.5
			Cu5-Bi1-Cu2-Cu3	59.4
$BiCu_4(C_{3v})$	Bi1-Cu2	2.569	Cu3-Bi1-Cu2	33.7
	Bi1-Cu3	4.075	Cu4-Bi1-Cu2	57.5
			Cu4-Bi1-Cu2-Cu3	−34.8
			Cu5-Bi1-Cu2-Cu3	34.8
$Bi_2Ag(C_{2v})$	Bi2-Ag1	2.807	Bi2-Ag1-Bi3	61.3
$BiAg_2(C_{2v})$	Bi3-Ag1	2.716	Ag1-Bi3-Ag2	64.2
$Bi_3Ag(C_s)$	Bi1-Bi2	2.815	Ag3-Bi1-Bi2	71.4
	Bi1-Ag3	4.404	Bi4-Bi1-Bi2	62.5
	Bi1-Bi4	3.046	Bi4-Bi1-Bi2-Ag3	−40.4
$Bi_2Ag_2(C_{2v})$	Bi1-Bi2	3.092	Ag3-Bi1-Bi2	57.5
	Bi1-Ag3	2.880	Ag4-Bi1-Bi2-Ag3	−70.8
$BiAg_3(C_{3v})$	Bi1-Ag2	2.737	Ag3-Bi1-Bi2	64.3
		2.914	Ag4-Bi1-Bi2-Bi3	72.4
$Bi_4Ag(C_s)$	Bi1-Bi2	4.006	Bi3-Bi1-Bi2	48.8
	Bi1-Bi3	3.040	Ag5-Bi1-Bi4	86.3
	Bi1-Ag5	2.838	Ag5-Bi1-Bi4-Bi2	27.9
			Bi4-Bi1-Bi2-Bi3	−82.3
$Bi_3Ag_2(C_1)$	Bi1-Bi2	3.032	Ag3-Bi1-Bi2	105.3
	Bi1-Ag3	2.858	Bi4-Bi2-Bi1	63.0
	Bi4-Bi2	2.992	Ag5-Ag3-Bi1	63.7
	Ag5-Ag3	2.788	Bi4-Bi2-Bi1-Ag3	−103.4
			Ag5-Ag3-Bi1-Bi2	44.5
$Bi_2Ag_3(C_s)$	Bi1-Ag2	2.836	Ag3-Bi1-Ag2	61.9
	Bi1-Bi4	3.183	Bi4-Bi1-Ag2	58.7
	Bi4-Ag5	2.812	Ag5-Bi1-Ag2	61.1
			Bi4-Bi1-Ag2-Ag3	68.6
			Ag5-Bi4-Ag2-Bi1	138.3

Table A.1. Continued.

Cluster(Sim)	Bond	Length	Angle	
$BiAg_4(C_{3v})$	Bi1-Ag2	2.776	Ag3-Bi1-Ag2	64.5
	Bi1-Ag3	2.811	Ag4-Ag3-Bi1	104.5
			Ag4-Ag3-Bi1-Ag2	−36.2
			Ag5-Bi1-Ag3-Ag4	36.2
$Bi_2Au(C_{2v})$	Bi2-Au1	2.761	Bi2-Au1-Bi3	63.4
$BiAu_2(C_{2v})$	Bi3-Au1	2.650	Au1-Bi3-Au2	73.3
$Bi_3Au(C_s)$	Bi1-Bi2	2.891	Au3-Bi1-Bi2	43.6
	Bi1-Au3	3.981	Bi4-Bi1-Bi2	83.3
	Bi1-Bi4	2.891	Bi4-Bi1-Bi2-Au3	−20.8
$Bi_2Au_2(C_{2v})$	Bi1-Bi2	4.240	Au3-Bi1-Bi2	37.7
	Bi1-Au3	2.680	Au4-Bi1-Bi2-Au3	180.0
$BiAu_3(C_{3v})$	Bi1-Au2	2.677	Au3-Bi1-Bi2	70.7
			Au4-Bi1-Bi2-Bi3	75.6
$Bi_4Au(C_{2v})$	Bi1-Bi2	4.037	Bi3-Bi1-Bi2	48.5
	Bi1-Bi3	3.045	Au5-Bi1-Bi4	84.4
	Bi1-Au5	2.775	Au5-Bi1-Bi4-Bi2	27.1
			Bi4-Bi1-Bi2-Bi3	−82.9
$Bi_3Au_2(C_{2v})$	Bi1-Bi2	3.067	Au3-Bi1-Bi2	48.5
	Bi1-Au3	3.534	Bi4-Bi1-Au3-Bi2	−122.7
			Au5-Bi1-Bi4-Au3	−79.0
$Bi_2Au_3(C_{3h})$	Bi1-Au2	2.782	Au3-Bi1-Au2	69.7
			Bi4-Au3-Bi1	97.4
			Bi4-Au3-Bi1-Au2	37.5
$BiAu_4(C_{3v})$	Bi1-Au2	2.711	Au3-Bi1-Au2	41.9
	Bi1-Au3	4.238	Au4-Bi1-Au2	70.7
			Au5-Bi1-Bi4-Au3	−37.8

References

1. Z.Y. Jiang, K.H. Lee, S.T. Li, S.Y. Chu, Phys. Rev. B **73**, 235423 (2006)
2. M. Zhang, L.M. He, L.X. Zhao, X.J. Feng, Y.H. Luo, J. Phys. Chem. C **113**, 6491 (2009)
3. S. Ganguly, M. Kabir, S. Datta, B. Sanyal, A. Mookerjee, Phys. Rev. B. **78**, 014402 (2008)
4. L. Leppert, S. Kümmel, J. Phys. Chem. C **115**, 6694 (2011)
5. J.J. Melko, U. Werner, R. Mitriæ, V. Bonaciæ-Koutecký, A.W. Castleman Jr., J. Phys. Chem. A **115**, 10276 (2011)
6. T.P. Martin, J. Chem. Phys. **83**, 78 (1985)
7. R. Ferrando, J. Jellinek, R.L. Johnson, Chem. Rev. **108**, 845 (2008)
8. E. Janssens, H. Tanaka, S. Neukermans, R.E. Silverans, P. Lievens, Phys. Rev. B **69**, 085402 (2004)
9. S. Heiles, R.L. Johnston, R. Schäfer, J. Phys. Chem. A **116**, 7756 (2012)
10. E.M. Fernández, J.M. Soler, I.L. Garzón, L.C. Balbás, Phys. Rev. B **70**, 165403 (2004)
11. H.K. Yuan, H. Chen, A.L. Kuang, Y. Miao, Z.H. Xiong, J. Chem. Phys. **128**, 094305 (2008)
12. A.N. Kuznetsov, L. Kloo, M. Lindsjö, J. Rosdahl, H. Stoll, Chem. Eur. J. **7**, 2821 (2001)
13. Y. Yamada, H.T. Deng, E.M. Snyder, A.W. Castleman Jr., Chem. Phys. Lett. **203**, 330 (1993)
14. M.J. Frisch, G.W. Trucks, H.B. Schlegel, G.E. Scuseria, M.A. Robb, J.R. Cheeseman, G. Scalmani, V. Barone, B. Mennucci, G.A. Petersson, H. Nakatsuji, M. Caricato, X. Li, H.P. Hratchian, A.F. Izmaylov, J. Bloino, G. Zheng, J.L. Sonnenberg, M. Hada, M. Ehara, K. Toyota, R. Fukuda, J. Hasegawa, M. Ishida, T. Nakajima, Y. Honda, O. Kitao, H. Nakai, T. Vreven, J.A. Montgomery Jr., J.E. Peralta, F. Ogliaro, M. Bearpark, J.J. Heyd, E. Brothers, K.N. Kudin, V.N. Staroverov, R. Kobayashi, J. Normand, K. Raghavachari, A. Rendell, J.C. Burant, S.S. Iyengar, J. Tomasi, M. Cossi, N. Rega, J.M. Millam, M. Klene, J.E. Knox, J.B.V. Cross, C. Bakken, C. Adamo, J. Jaramillo, R. Gomperts, R.E. Stratmann, O. Yazyev, A.J. Austin, R. Cammi, C. Pomelli, J.W. Ochterski, R.L. Martin, K. Morokuma, V.G. Zakrzewski, G.A. Voth, P. Salvador, J.J. Dannenberg, S. Dapprich, A.D. Daniels, O. Farkas, J.B. Foresman, J.V. Ortiz, J. Cioslowski, D.J. Fox, *Gaussian 09, Revision A.02* (Gaussian, Inc., Wallingford CT, 2009)
15. B. Metz, H. Stoll, M. Dolg, J. Chem. Phys. **113**, 2563 (2000)
16. D. Andrae, U. Haeussermann, M. Dolg, H. Stoll, H. Preuss, Theor. Chem. Acc. **77**, 123 (1990)
17. Y. Zhao, D.G. Truhlar, J. Chem. Phys. **125**, 194101 (2006)
18. J. Pérez, A. Restrepo, *ASCEC V-02: Annealing Simulado con Energía Cuántica. Property, development and implementation* (Grupo de Química-Física Teórica, Instituto de Química, Universidad de Antioquia, Medellín, Colombia, 2008)
19. J. Cizek, Adv. Chem. Phys. **14**, 35 (1969)
20. G.D. Purvis, R.J. Bartlett, J. Chem. Phys. **76**, 1910 (1982)
21. G.E. Scuseria, C.L. Janssen, H.F. Schaefer III, J. Chem. Phys. **89**, 7382 (1988)
22. G.E. Scuseria, C.L. Janssen, H.F. Schaefer III, J. Chem. Phys. **89**, 7382 (1988)
23. J.A. Pople, M. Head-Gordon, K. Raghavachari, J. Chem. Phys. **87**, 5968 (1987)
24. C. Effantin, A. Topouzkhanian, J. Figuet, J. d'Incan, R.F. Barrow, J. Vergés, J. Phys. B **15**, 3829 (1982)
25. K.P. Huber, G. Herzberg, *Molecular Spectra and Molecular Structure, IV. Constants of Diatomic Molecules* (Van Nostrand, New York, 1979)
26. Q. Sun, P. Jena, Y.D. Kim, M. Fischer, G. Ganteför, J. Chem. Phys. **120**, 6510 (2004)
27. S. Li, M.M.G. Alemany, J.R. Chelikowsky, J. Chem. Phys. **125**, 034311 (2006)
28. S. Lecoultre, A. Rydlo, C. Félix, J. Buttet, S. Gilb, W. Harbich, J. Chem. Phys. **134**, 074303 (2011)
29. P. Fuentealba, P. Pérez, R. Contreras, J. Chem. Phys. **113**, 2544 (2000)
30. Z. Chen, C. Corminboeuf, T. Heine, J. Bohmann, P.V.R. Schleyer, J. Am. Chem. Soc. **125**, 13930 (2003)
31. K. Ruud, T. Helgaker, K.L. Bak, P. Jorgensen, H.J.A. Jensen, J. Chem. Phys. **99**, 3847 (1993)
32. A.I. Boldyrev, L.S. Wang, Chem. Rev. **105**, 3716 (2005)
33. Z. Li, C. Zhao, L. Chen, J. Mol. Struct. (Theochem) **854**, 46 (2008)